Nanoholes on Silicon Surface Created by Electron Irradiation under Ultrahigh Vacuum Environment

S. Takeda and K. Koto
Department of Physics, Graduate School of Science, Osaka University, 1-16 Machikane-yama, Toyonaka, Osaka 560, Japan

S. Iijima and T. Ichihashi
Fundamental Research Laboratory, NEC, Miyuki-cho, Tsukuba, Ibaraki, Japan
(Received 7 April 1997)

We have found that a novel structure is formed in a thin silicon crystal. Uniform-intensity electron irradiation in an ultrahigh vacuum environment (1.0×10^{-7} Pa) introduces an array of holes 2 to 3 nm in diameter and several nanometers deep at the electron exit surfaces. The holes are distributed in average 6 nm apart. The irradiation temperature is needed to be below 300 °C. The formation of the holes occurs regardless of the surfaces, i.e., {111} and {110}. It is suggested that the phenomenon is attributed to the spinodal instability involving the surface vacancies accumulated by electron irradiation. [S0031-9007(97)04242-7]

PACS numbers: 61.72.Ff, 61.80.Fe, 68.55.Ln, 81.05.Cy

Silicon is the most important crystalline material from both fundamental and technological points of view. The recent interests focus on fabricating the structurally and/or chemically heterogeneous silicon-related materials in nanometer dimension such as porous silicon, silicon wires, and artificial superlattices, which may exhibit novel physical properties such as quantum confinement. Transmission electron microscopy (TEM) is a useful means of characterizing the materials in nanometer dimension. This imaging technique has two other aspects; implicitly, an observation by TEM and related techniques itself leads to a discovery of a new structure as recently shown [1,2] and the materials under observation are heavily irradiated by accelerated electrons. In this Letter, we report that the entirely novel phenomenon in Si crystal is induced by electron irradiation during TEM observation. An array of holes a few nanometers in diameter and several nanometers deep is created at the electron exit surface in an ultrahigh vacuum environment. Unlike the previous attempts to fabricate nanostructures by a focused electron beam [3], the phenomenon is caused by the uniform-intensity electron irradiation. We attribute the formation of the array of holes to the spinodal instability involving surface vacancies which are accumulated by electron irradiation. The phenomenon has potential applications in the formation of nanometer-scale structures in Si and other semiconductors for future microelectronic works.

The specimens are nondoped floating zone-melting (FZ) {111} and Czochralski (CZ) {110} Si. Disks of 3 mm in diameter were mechanically prepared using an ultrasonic drill. The center of a disk was dimpled and then etched in the mixed solution of HNO_3 and HF until the center of the disk was transparent for visible light. The disk was heated in a pretreatment chamber of an ultrahigh vacuum (UHV)-TEM [4] (Jeol JEM2000FXV) by illumination of infrared light at about 1200 °C for several minutes. The heating process provides the thermally etched flat terraces on both sides of the disk and consequently a number of parallel-sided thin slabs of 10 to several 100 nm thickness were created. The base pressure in the UHV-TEM was estimated to be 1.0×10^{-7} Pa. The electron energy for intense irradiation, E_r, was 141, 160, and 200 keV. The irradiation directions were nearly parallel to the ⟨111⟩ and ⟨110⟩ zone axes, respectively, for the {111} and {110} disks. The electron flux in irradiation was equal to $3.5 \times 10^{21} e\ \mathrm{cm}^{-2}\,\mathrm{s}^{-1}$. The specimen temperature during irradiation, T_r, was set at 200, 300, and 400 °C. The specimen temperature was estimated by measuring the heating current, based on the calibrating data which was determined prior to the observations by pyrometry. While O_2 flowed in the specimen chamber in order to modify surfaces of a specimen, the estimated pressure was kept at 5.0×10^{-5} Pa. The thicknesses of the observed slabs were measured by a convergent beam electron diffraction (CBED) technique using a conventional TEM (Jeol JEM2010) after the UHV-TEM observations. The thicknesses in the following observations ranged from 30 to 50 nm, and no change was found in experimental results depending on the thickness.

Figures 1(a) to 1(c) depict the formation process of nanoholes revealed by *in situ* UHV-TEM observation. During irradiation, the electron beam of uniform intensity covers the central area of about 100 nm in diameter in Fig. 1(a). After irradiation for 300 s [Fig. 1(b)], the fuzzy bright spots appear in the irradiated area. The contrast of the spots is gradually enhanced with the increase of irradiation time [Fig. 1(c)]. The spots are linked by the fainter bandlike contrasts. The locations and sizes of these contrasts are kept unchanged under irradiation [Figs. 1(b) to 1(c)]. The contrast of the spots changes with the defocus setting of the objective lens [Figs. 1(d) and 1(e)]. The change arises from the Fresnel diffraction effect [5] and accordingly we conclude that hollow spaces are created

 0031-9007/97/79(16)/2994(4)$10.00

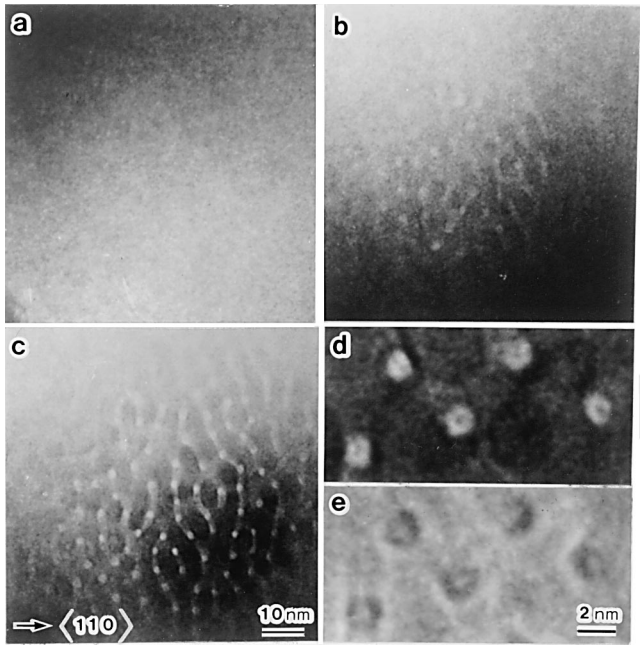

FIG. 1. Formation of the nanohole array on a Si surface [$E_r = 141$ keV, $T_r = 200\,^{\circ}$C, CZ Si (110)]. Irradiation times were 0, 300, and 900 s in (a), (b), and (c), respectively. The enlarged images in (d) and (e) were taken after the irradiation with the under-focused (about -300 nm) and over-focused (about $+300$ nm) conditions, respectively.

either inside the thin foil or at the surfaces. A simple three-dimensional TEM observation (so called stereo microscopy) using the conventional TEM shows that the spot contrasts locate near the electron exit surface, which is slightly concave due to homogeneous sputtering of atoms in the electron irradiated area as has been described [6]. The irradiated areas are observed in several directions as well as the irradiation direction, and the spot contrasts are slightly elongated along the irradiation direction. These geometrical analyses have led to a conclusion that the holes of 2 to 3 nm diameter and 5 to 10 nm depth are created on the electron exit surfaces.

Figure 2(a) depicts an UHV high-resolution (HR)-TEM image of an area after electron irradiation in an UHV environment. The holes are separated by 6 nm in average and, in the Fourier transform of the image in (a), the corresponding diffuse rings appear around the origin and the fundamental diffraction spots. In an enlarged UHV-HRTEM image in Fig. 2(b), the holes exhibit the facets of {111} and {100} which are parallel to the irradiation direction. We attribute the fainter bandlike contrasts to shallow grooves on the surface.

The same phenomenon is induced by irradiation of electrons whose energy ranges from 141 to 200 keV. Because of the restriction on the accelerating voltages of electrons in the UHV-TEM, the threshold electron energy has not yet been determined. The formation of holes and grooves is irrelevant to Frenkel pairs created inside the crystal by electron irradiation, since the threshold electron

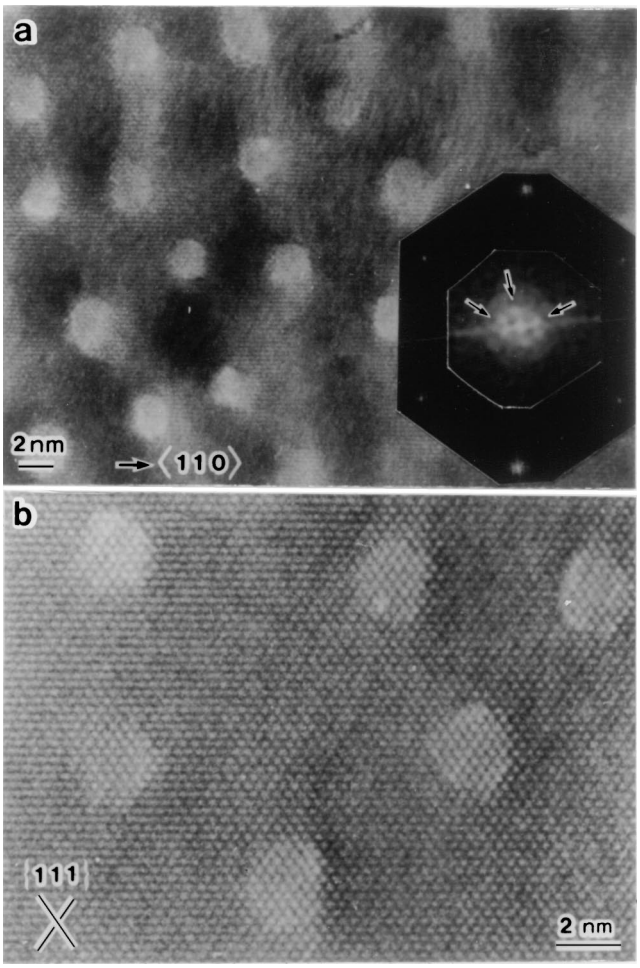

FIG. 2. Nanohole array on a Si surface [$E_r = 200$ keV, $T_r = 200\,^{\circ}$C, CZ Si (110)]. (a) Lower magnified image. The inset shows the Fourier transform of the image in (a). The central part is enlarged by 3 times so that the diffuse ring can be seen. The peaks appear in the ring as indicated by the arrows but their positions are not related to the crystal lattice. (b) A higher magnified image.

energy to create the pairs is about 150 keV [7]. When the specimens undergo the irradiation of electrons whose energy exceeds the threshold energy, the nanoholes and nanogrooves at the surface were created as well as the numerous {113} planar interstitial defects inside the crystal, which are definitely due to the Frenkel pair formation inside the crystal [8–10].

For observing the phenomenon, the irradiation temperature needs to be below 300 °C. Figure 3 summarizes the size distribution of the holes depending on various experimental conditions. As shown in Figs. 3(a) and 3(b), the hole formation is almost suppressed at 300 °C. Actually, we have never observed the hole formation above 400 °C. The Si surface at the lower temperature range is not well maintained thermally [11] and far away from the equilibrium, to which therefore less attention has been paid.

Figure 4 shows the UHV-TEM images taken from the 3 sequences of experiments with different vacuum

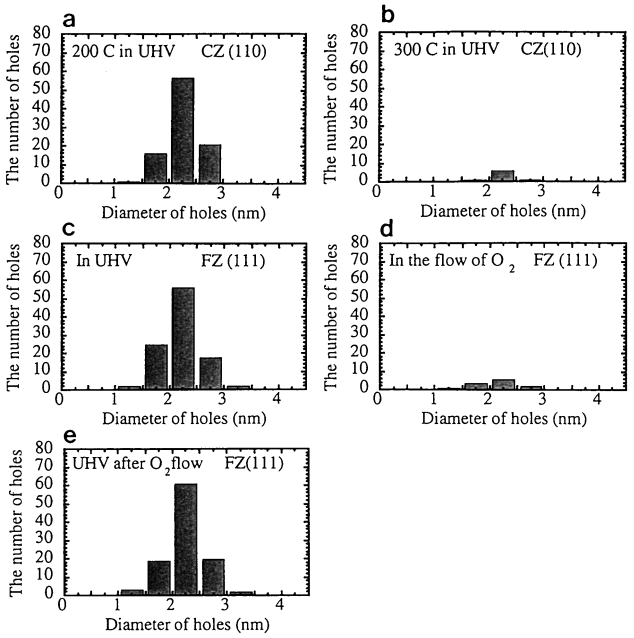

FIG. 3. The size distribution of nanoholes depending on various experimental conditions ($E_r = 200$ keV). The specimens received the same dose, i.e., 3.1×10^{24} cm^{-2}.

environments. After we observed the hole formation in the UHV condition [Fig. 4(a)], the O_2 gas was injected in the UHV specimen chamber. Then the irradiation proceeded on another area in the same specimen under the flow of O_2 gas. Clearly, the generation of holes was very suppressed [Fig. 4(b)]. The pressure at the specimen during the flow

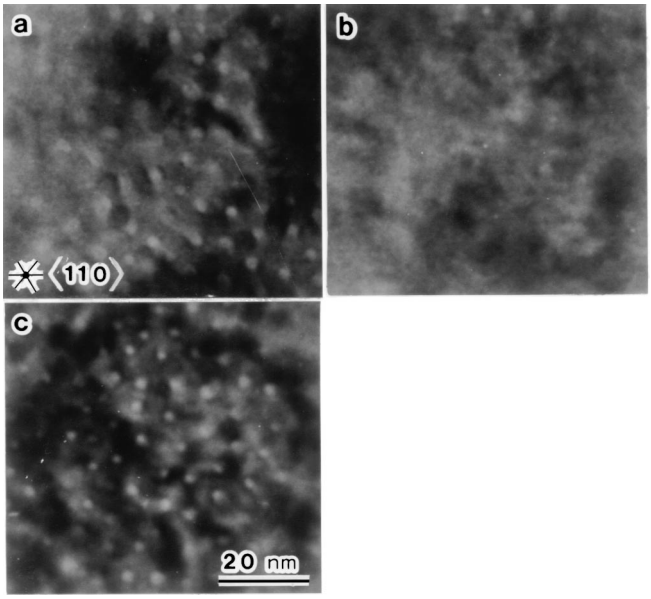

FIG. 4. The effect of the O_2 flush on the hole generation [$E_r = 200$ keV, $T_r = 200$ °C, FZ Si (111)]. (a) In UHV, (b) in the flow of O_2, and (c) in UHV after the interruption of the flow of O_2. The irradiation time is 900 s. The three crossed lines in (a) indicate the ⟨110⟩ directions.

of O_2 was comparable to that in a conventional TEM. In the last series, the irradiation commenced on another area in the same specimen, 1800 s after the interruption of the flow of O_2; the pressure was restored to better than 5×10^{-7} Pa. The holes and grooves were created again [Fig. 4(c)]. The size distribution of holes in the 3 series of experiments is summarized in Figs. 3(c), 3(d), and 3(e). From the experimental evidence, we conclude that the formation of holes and grooves is a surface-related phenomenon under electron irradiation. The holes and grooves are generated regardless of the surfaces, i.e., {111} and {110} and the content of oxygen, i.e., FZ and CZ [Figs. 3(a) and 3(c)].

Nucleation of the somewhat similar but more complicated structures has been reported in α-Al_2O_3 [12] and Au [6,13]. In the observations, the materials with uncontrolled surfaces were irradiated by electrons under conventional vacuum environment, and the role played by the surface could not be described experimentally. Our observation has clarified the effect of the surfaces on the phenomenon. More importantly, it has been shown that the generation of holes in a thin foil occurs generally in semiconductors as well as metals and oxides regardless of the nature of cohesion.

Let us discuss briefly the mechanism of the novel self-organized phenomenon. The momentum transfer from electrons to a thin foil induces sputtering of atoms from the electron exit surface [6], and a large number of vacancies are accumulated near and at the surface at the steady state. Surface vacancies likely agglomerate whenever they are movable, reducing the kinks and steps of higher energy. It is known that under ion bombardment in the UHV environment, surface vacancies are movable at the lower temperature [14,15]. Furthermore, under electron irradiation, more sluggish vacancies inside the crystal are movable far below the room temperature [16] presumably due to ionization. Hence, it is suggested that surface vacancies are responsible to the phenomenon. Considering the distribution of movable vacancies and atoms on a surface, a two-dimensional Ising model is naturally connected to the system. According to the picture, surface vacancies tend to agglomerate at lower temperatures, while at higher temperatures the random distribution of surface vacancies is expected, which may lead to the homogeneous surface structure [Fig. 3(b)]. Below the critical temperature, we expect a spinodal instability in the system [17], with which a morphology of vacancy agglomerates evolves in time. The spinodal decomposition can be definable under electron irradiation [18], and the microstructures driven by the instability [19] and the related one [20,21] are observable in several metallic alloys. It is suggested that the steady state under irradiation has the similar configuration as a transient state evolved from the quenched system [22]. Therefore, we refer to an early work by a Monte Carlo simulation [23] which described the time evolution in a quenched two-dimensional system. Small islands of the

minority species are nucleated, in the somewhat similar manner as the observation (Fig. 1), without coarsening of them when the fraction of minority species is 20%. The fraction of surface vacancies at the early stage in our observation is roughly estimated to be 30% [24], which is like that of the minorities. Hence, the spacial pattern of the holes is attributed to "spinodal decomposition" involving the accumulated surface vacancies in the steady state under the uniform-intensity electron irradiation. During the flow of O_2 [Fig. 4(b)], oxygen is absorbed on surfaces, and at the lower temperatures the oxidation proceeds heterogeneously after the early stage [25], preventing the surface vacancies from migrating freely. Consequently, the formation of the patterns is interrupted.

Subsequent irradiation in UHV induces further sputtering to expose the surfaces of lower energy as the walls of a hole [as seen in Fig. 2(b)]. Once the initial morphology is set up, the holes may be deepened under irradiation, since the mass must flow preferentially from the lower surfaces (the bottom surfaces of the holes) to the higher surface; the surface vacancies must flow preferentially in the reverse direction along the wall of the holes.

In summary, besides the ongoing arguments on the nucleation mechanism, we have shown for the first time that the nanoholes are created on the electron exit surfaces in Si by the uniform-intensity electron irradiation in the UHV environment. We have found the narrow experimental window through which the novel phenomenon of a silicon thin crystal can be observed. The finding could be utilized for fabricating nanometer-scale structures in Si and other semiconductors in many ways.

This work is in part supported by the Grant-in-Aid from the Ministry of Education, Science, Sports and Culture, to which the author (S. T.) is grateful.

[1] D. Shechtman, I. Blech, D. Gratias, and J. W. Cahn, Phys. Rev. Lett. **53**, 1951 (1984).
[2] S. Iijima, Nature (London) **354**, 56 (1991).
[3] G. S. Chen, C. B. Boothroyd, and C. J. Humphreys, Appl. Phys. Lett. **62**, 1949 (1993).
[4] E. Bengu, R. Plass, L. D. Marks, T. Ichihashi, P. M. Ajayan, and S. Iijima, Phys. Rev. Lett. **77**, 4226 (1996).
[5] For example, S. Horiuchi, *Fundamentals of High-Resolution Transmission Electron Microscopy* (North-Holland, Amsterdam, 1994).
[6] D. Cherns, Surf. Sci. **90**, 336 (1979).
[7] J. J. Loferski and P. Pappaport, Phys. Rev. **111**, 432 (1958).
[8] C. A. Ferreira Lima and A. Howie, Philos. Mag. **34**, 1057 (1976).
[9] I. G. Salisbury and M. H. Loretto, Philos. Mag. A **39**, 317 (1979).
[10] S. Takeda, Jpn. J. Appl. Phys. **30**, L639 (1991).
[11] D. J. Eaglesham, H.-J. Gossmann, and M. Cerullo, Phys. Rev. Lett. **65**, 1227 (1990).
[12] Y. Tomokiyo, T. Kuroiwa, and C. Kinoshita, Ultramicroscopy **39**, 213 (1991).
[13] K. Niwase, W. Sigle, F. Phillip, and A. Seeger, Philos. Mag. Lett. **74**, 167 (1996).
[14] P. Bedrossian, J. E. Houston, J. Y. Tsao, E. Chason, and S. T. Picraux, Phys. Rev. Lett. **67**, 124 (1991).
[15] P. Bedrossian and T. Klitsner, Phys. Rev. B **44**, 13 783 (1991).
[16] G. D. Watkins, Inst. Phys. Conf. Ser. **23**, 1 (1975).
[17] H.-J. Ernst, F. Fabre, and J. Lapujoulade, Phys. Rev. Lett. **69**, 458 (1992).
[18] G. Martin, Phys. Rev. B **30**, 1424 (1984).
[19] K. Nakai and C. Kinoshita, J. Nucl. Mater. **169**, 116 (1989).
[20] S. Banerjee, K. Urban, and M. Wilkens, Acta Metall. **32**, 299 (1984).
[21] J. Mayer and K. Urban, Acta Metall. **33**, 539 (1985).
[22] S. Takeda, J. Kulik, and D. de Fontaine, Acta Metall. **35**, 2243 (1987).
[23] M. Rao, M. H. Kalos, J. L. Lebowitz, and J. Marro, Phys. Rev. B **13**, 4328 (1976).
[24] The ratio of vacancies on a surface can roughly be estimated as $(\pi/\sqrt{3})(\overline{r}/\overline{L})^2$ using the average radius $\overline{r}$ and the average distance $\overline{L}$ of vacancy islands. The values are experimentally deduced from Fig. 2 as $\overline{r} = 2.5$ nm and $\overline{L} = 6.0$ nm.
[25] T. Hasegawa, M. Kohno, S. Hosaka, and S. Hosoki, Surf. Sci. **312**, L753 (1994).